ChemComm

COMMUNICATION

View Article Online
View Journal | View Issue

Cite this: *Chem. Commun.*, 2025, **61**, 3998

Received 27th December 2024,
Accepted 5th February 2025

DOI: 10.1039/d4cc06751g

rsc.li/chemcomm

Liquid-crystalline nanostructured membranes for CO_2 separation†

Takashi Kato, *[ab] Kazushi Imamura,[c] Takeshi Sakamoto [a] and Yu Hoshino*[c]

We report herein that self-organized subnanoporous membranes prepared from ionic liquid-crystalline (LC) compounds exhibit CO_2 separation properties ($\alpha CO_2/N_2 \approx 60$) in humid conditions. A bicontinuous cubic (Cub_{bi}) LC film shows N_2 barrier properties, whereas the CO_2 permeability is kept as permeable.

The development of CO_2 separation membranes[1–3] that allow rapid and selective CO_2 permeation is critical for rebalancing the global carbon cycle.[4] Membranes fabricated from polymers,[5–8] graphene oxide,[9] metal–organic frameworks,[10] zeolites,[11] organic/inorganic interpenetrating networks,[12] and liquid water[13] have been prepared for CO_2 gas separation. To achieve optimal performance, defect-free ultrathin separation membranes enabling fast sorption, diffusion, and desorption of CO_2 need to be designed, while minimizing the sorption of competing gases.

Thin films derived from polyamine-based hydrogel particles[14–16] and gel membranes of ionic liquids[17–19] were also examined for CO_2 separation. Since the humidity of gas strongly affects its permeability through polymer membranes,[7,14–20] gas permeation behaviors under various humid conditions were examined. Poly(ionic liquid) membranes have been shown to be useful for CO_2 separation.[17] These materials contain ionic groups such as ammonium, imidazolium, and phosphonium moieties. However, these membranes form basically amorphous states.[17–19] We expected that the self-organized structures of ionic subnanoporous membranes[21–25] in humid conditions may enhance the gas separation properties. These structures are fixed by *in situ* polymerization of ionic liquid-crystalline (LC) compounds in the ordered state.

Our intention was to develop self-organized ionic LC membranes[21–29] for CO_2 gas separation. Several examples were reported as LC gas separation membranes.[30–32] Bara *et al.* reported CO_2 permeation through the membrane prepared from a lyotropic columnar LC monomer having a carboxylic acid moiety.[30] The membrane with an ordered cylinder structure showed higher CO_2 separation properties ($\alpha CO_2/N_2 \approx 27$) compared to the non-ordered membrane prepared from the isotropic phase ($\alpha CO_2/N_2 \approx 21$). It was assumed that interactions between CO_2 and the carboxylate groups of the ordered membrane with the aquatic environment of the pores caused higher CO_2 solubility and gas separation. Kloos *et al.* described gas separation using a smectic polymer membrane prepared from rod-shaped monomers having a crown ether moiety.[31] The membranes preserving more ordered smectic structures showed CO_2/N_2 separation properties whereas membranes having disordered structures did not exhibit the gas separation.[31] Jones *et al.* reported lyotropic liquid crystals showing light-driven columnar-to-cubic phase switching and the phase transition changed their CO_2 permeability.[32] Development of membranes with ordered pores and the examination of the relationship between the organized structures and performance of the membranes are of interest.

Here, we describe the CO_2 gas separation properties of subnanoporous LC membranes in high humidity conditions. A wedge-shaped LC compound (**1**) and a rod-shaped LC compound (**2**) (Fig. 1) were used for the evaluation of gas permeation. These polymer films were originally developed as ion-conductors[26–29,33] and water-treatment membranes.[21–25] Compound **1** exhibits a bicontinuous cubic (Cub_{bi}) phase and its nanostructured membrane shows salt rejection comparable to those of nanofiltration membranes.[21,22] Compound **2** forms smectic (Sm) phases exhibiting two-dimensional channels showing enhanced water permeability and lower salt rejection ability since the Sm phase shows larger ratio of the hydrophilic nanopores.[23]

The ionic LC membranes show unique ion permeation/rejection selectivity due to interactions among the ionic moieties, solutes, and water molecules.[21,22,34–37] It is of interest to

[a] *Department of Chemistry and Biotechnology, School of Engineering, The University of Tokyo, 7-3-1 Hongo, Bunkyo-ku, Tokyo 113-8656, Japan. E-mail: kato@chiral.t.u-tokyo.ac.jp*
[b] *Institute for Aqua Regeneration, Shinshu University, 4-17-1 Wakasato, Nagano 380-8553, Japan*
[c] *Department of Applied Chemistry, Kyushu University, 744 Motooka, Nishi-ku, Fukuoka 819-0395, Japan. E-mail: hoshino.yu.673@m.kyushu-u.ac.jp*

† Electronic supplementary information (ESI) available. See DOI: https://doi.org/10.1039/d4cc06751g

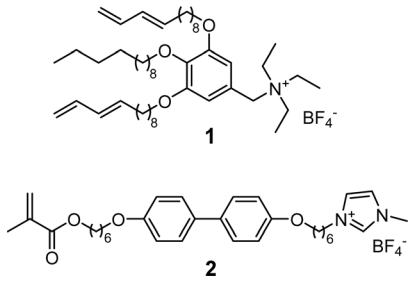

Fig. 1 Molecular structures of the LC monomers.

examine the performance of those organized ionic sites for CO_2 separation.

Compounds **1** and **2** (Fig. 1) were synthesized according to the procedures previously reported.[21–24] Polymer membranes (**P1** and **P2**) for the gas separation tests were prepared from the LC monomers **1** and **2**, respectively, with the transcription method using a poly(vinyl alcohol) (PVA) layer as a sacrifice layer (Fig. S1, ESI†).[21] On a PVA substrate, compound **2** forms vertically aligned nanochannels in the Sm phase.[25] Thin films of **1** or **2** were obtained by *in situ* polymerization of the spin-coated mixture of the monomer and a photoinitiator on the PVA substrate. The nanostructured LC polymer layer was supported by porous substrates composed of polysulfone and poly(ethylene terephthalate) (PET) (Fig. 2). These supporting layers impart mechanical toughness to the membranes.

The gas-permeation properties of the LC membranes (diameter = 25 mm) were evaluated by flowing simulated post-combustion gases containing 10 vol% CO_2 and 90 vol% N_2 (40 °C, 100 mL min^{-1}) on the top side of the membranes of the LC polymer film (Fig. S2, ESI†). The gas mixture was humidified by passing through a temperature-controlled water bath. The backside of the membranes was swept with helium gas to

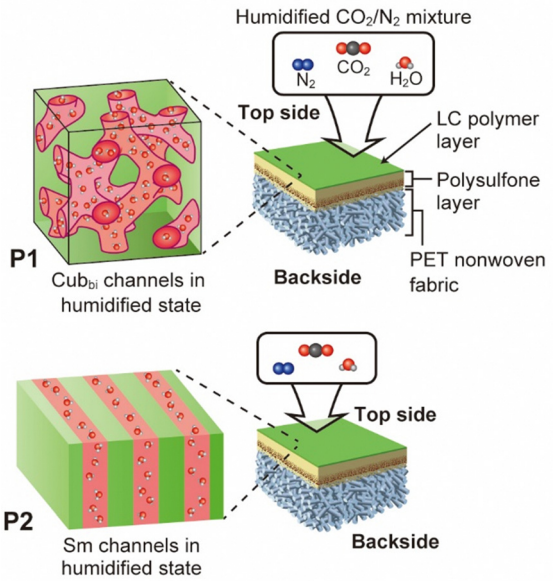

Fig. 2 Schematic illustrations of the nanostructured LC polymer membranes in controlled humid conditions.

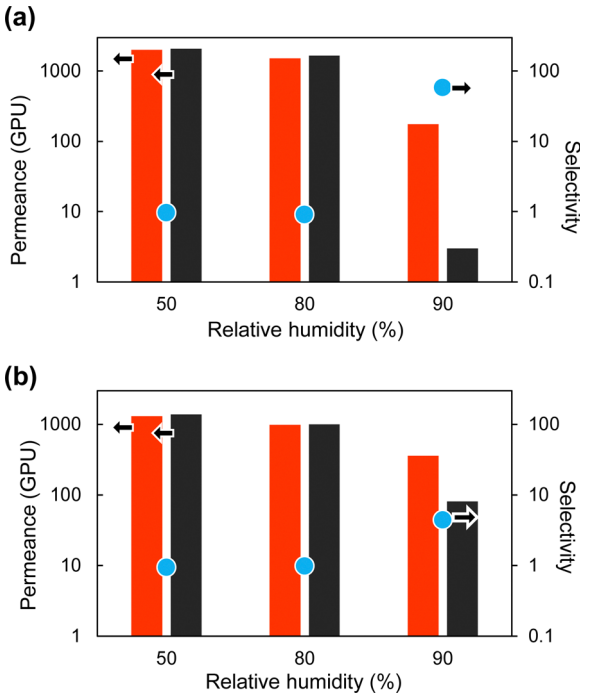

Fig. 3 Effects of humidity on CO_2 (red bars), N_2 (black bars) permeance and selectivity (blue dots) of (a) **P1** and (b) **P2** LC membranes at 40 °C.

quantify the amount of gaseous species in the permeate by gas chromatography. The humidity of the backside gas was also controlled so that the gas humidity on both sides was the same.

Fig. 3 shows the permeance of CO_2 and N_2 permeation through **P1** and **P2** membranes when the relative humidity (RH) of the supplied gas was set to 50%, 80%, and 90%. **P1** and **P2** membranes showed high CO_2 and N_2 permeance below 80% RH. The permeances of CO_2 and N_2 were calculated to be of over 1000 gas permeation units (GPU, where 1 GPU = 1×10^{-6} cm^3(STP) ($s\ cm^2\ cmHg)^{-1}$). The CO_2 selectivity, $\alpha CO_2/N_2$ (permeance of CO_2/permeance of N_2) was almost 1, indicating that these membranes did not work as CO_2 separation membranes below 80% RH.

The N_2 permeance of the Cub_{bi} membrane **P1** decreased dramatically from 1500 GPU to 3 GPU when the humidity was increased from 80% RH to 90% RH (Fig. 3a). The N_2 permeance through the **P2** membrane also decreased under high humidity, but it was about 80 GPU (Fig. 3b). The N_2 barrier property of the smectic **P2** membrane was approximately 1/30th that of Cub_{bi} **P1** membrane. The CO_2 permeance also decreased when increasing the RH from 80% to 90%. However, the CO_2 permeances through the sub-nanoporous membranes were greater than those of N_2 for each membrane and the CO_2 permeance was almost independent from the structures of **P1** and **P2** in contrast to the N_2 permeance. The CO_2 permeance of the **P1** membrane was about 180 GPU and that of **P2** was about 360 GPU at 90% RH, respectively. Consequently, these LC membranes exhibited CO_2 selectivity under humid conditions. In particular, the Cub_{bi} **P1** membrane at 90% RH showed the highest CO_2 selectivity ($\alpha CO_2/N_2 \approx 60$). This reflects the high

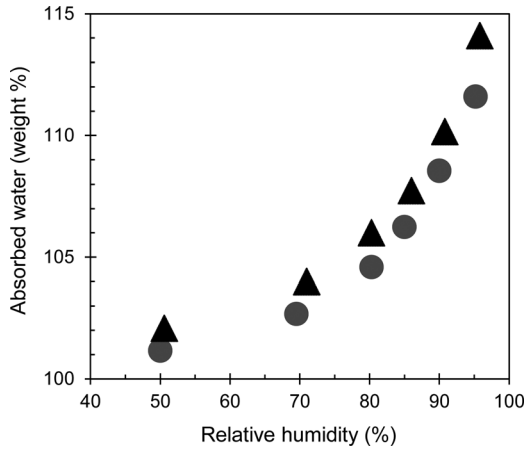

Fig. 4 Effect of humidity on the amount of water absorbed by **P1** (Cub_{bi}) (triangle) and **P2** (Sm) (circle) membranes at 40 °C.

N_2 barrier performance of the Cub_{bi} membranes under high humidity conditions.

Since post-combustion exhaust gas has a high water vapor partial pressure with a humidity of over 90% RH, the development of CO_2 separation membranes that function at high humidity is important, and thus various membranes for such purpose have been reported.[7,9,14–20,38–40] Typically, membranes such as amine-added membranes and hydrogel membranes absorb water at high humidity, and the absorbed water facilitates CO_2 to dissolve and diffuse in the membrane.[7,14–16,19,20,40] On the other hand, since N_2 has low polarity, its solubility in membranes decreases due to moisture absorption by the membrane. The high CO_2 selectivity that appeared in the LC membrane under high humidity is due to the low solubility of N_2 caused by moisture absorption by the ionic liquid crystal, while the solubility of highly polar CO_2 was maintained. The differences in N_2 barrier properties and CO_2 selectivity under high humidity between liquid crystal membranes with different phases may be due to the efficiency of their ionic moieties. It is assumed that the effects of ionic moieties are further critical in the Cub_{bi} structure with smaller nanochannels compared to the Sm structure shown as their ion removal properties.[21,23]

To clarify the cause of the difference in gas permeance of **P1** and **P2** membranes at high humidity, we quantified the amount of water absorbed by the **P1** and **P2** membranes under highly humidified conditions with a thermogravimetry differential thermal analysis system equipped with a humidity controller (TG-DTA/HUM, Fig. S3, ESI†). For the TG-DTA/HUM measurements, nanostructured polymer membranes without the polysulfone substrate were used. Fig. 4 shows the mass changes of each membrane. Both the membranes **P1** (Cub_{bi}) and **P2** (Sm) absorbed water when the humidity was gradually increased at 40 °C. They absorbed water by weight of approximately 10% of the dry weight of the membrane at 90% RH. The amount of absorbed water was not significantly different between the Cub_{bi} and Sm films. This indicates that under high humidity, the polarity of the membrane increases as the membrane absorbs water, and as a result the solubility of N_2, which is non-polar, decreases, resulting in an increase in barrier properties against N_2.

In conclusion, we have found that an ionic self-organized membrane that preserves a bicontinuous LC cubic structure exhibits the CO_2/N_2 selectivity of 60 at 90% RH, whereas no selectivity was observed below 80% RH. This selectivity at higher humidity is caused by water molecules adsorbed in the ionic subnanoporous membranes, which disturb the permeation of non-polar N_2 molecules.

T. K. and Y. H. conceived and designed the project. T. K., K. I., T. S. and Y. H. wrote the manuscript. T. S. synthesized the LC molecules and prepared the LC membranes. K. I. performed the gas separation experiments and analyzed the data. All of the authors read the paper.

This work was supported by a JSPS KAKENHI (JP19H05715; Grant-in-Aid for Scientific Research on Innovative Areas of Aquatic Functional Materials). This research was also supported by the MEXT Program, Data Creation and Utilization-Type Material Research and Development Project (Grant Number JPMXP1122714694), and JST (Grant Number JPMJPF2114).

Data availability

The data supporting this article have been included as part of the ESI.†

Conflicts of interest

There are no conflicts to declare.

Notes and references

1 K. Xie, Q. Fu, G. G. Qiao and P. A. Webley, *J. Membr. Sci.*, 2019, **572**, 38.
2 Y. Fan, W. Yu, A. Wu, W. Shu and Y. Zhang, *RSC Adv.*, 2024, **14**, 20714.
3 N. Du, H. B. Park, M. M. Dal-Cin and M. D. Guiver, *Energy Environ. Sci.*, 2012, **5**, 7306.
4 T. C. Merkel, H. Lin, X. Wei and R. Baker, *J. Membr. Sci.*, 2010, **359**, 126.
5 Y. Hirayama, T. Yoshinaga, Y. Kusuki, K. Ninomiya, T. Sakakibara and T. Tamari, *J. Membr. Sci.*, 1996, **111**, 169.
6 M. F. Jimenez-Solomon, Q. Song, K. E. Jelfs, M. Munoz-Ibanez and A. G. Livingston, *Nat. Mater.*, 2016, **15**, 760.
7 Y. Chen and W. S. W. Ho, *J. Membr. Sci.*, 2016, **514**, 376.
8 Z. Qiao, S. Zhao, M. Sheng, J. Wang, S. Wang, Z. Wang, C. Zhong and M. D. Guiver, *Nat. Mater.*, 2019, **18**, 163.
9 H. W. Kim, H. W. Yoon, S.-M. Yoon, B. M. Yoo, B. K. Ahn, Y. H. Cho, H. J. Shin, H. Yang, U. Paik, S. Kwon, J.-Y. Choi and H. B. Park, *Science*, 2013, **342**, 91.
10 Y. Wang, H. Jin, Q. Ma, K. Mo, H. Mao, A. Feldhoff, X. Cao, Y. Li, F. Pan and Z. Jiang, *Angew. Chem., Int. Ed.*, 2020, **59**, 4365.
11 M. Y. Jeon, D. Kim, P. Kumar, P. S. Lee, N. Rangnekar, P. Bai, M. Shete, B. Elyassi, H. S. Lee, K. Narasimharao, S. N. Basahel, S. Al-Thabaiti, W. Xu, H. J. Cho, E. O. Fetisov, R. Thyagarajan, R. F. DeJaco, W. Fan, K. A. Mkhoyan, J. I. Siepmann and M. Tsapatsis, *Nature*, 2017, **543**, 690.
12 R. Vendamme, S. Onoue, A. Nakao and T. Kunitake, *Nat. Mater.*, 2006, **5**, 494.
13 Y. Fu, Y. B. Jiang, D. Dunphy, H. Xiong, E. Coker, S. S. Chou, H. Zhang, J. M. Vanegas, J. G. Croissant, J. L. Cecchi, S. B. Rempe and C. J. Brinker, *Nat. Commun.*, 2018, **9**, 990.
14 Y. Hoshino and S. Aki, *Polym. J.*, 2024, **56**, 463.

15 Y. Hoshino, T. Gyobu, K. Imamura, A. Hamasaki, R. Honda, R. Horii, C. Yamashita, Y. Terayama, T. Watanabe, S. Aki, Y. Liu, J. Matsuda, Y. Miura and I. Taniguchi, *ACS Appl. Mater. Interfaces*, 2021, **13**, 30030.
16 Y. Liu, D. Nakamura, J. Gao, K. Imamura, S. Aki, Y. Nagai, I. Taniguchi, K. Fujiwara, R. Horii, Y. Miura and Y. Hoshino, *ACS Appl. Mater. Interfaces*, 2024, **16**, 29112.
17 M. G. Cowan, D. L. Gin and R. D. Noble, *Acc. Chem. Res.*, 2016, **49**, 724.
18 Z. Dai, L. Ansaloni, D. L. Gin, R. D. Noble and L. Deng, *J. Membr. Sci.*, 2017, **523**, 551.
19 F. Moghadam, E. Kamio and H. Matsuyama, *J. Membr. Sci.*, 2017, **525**, 290.
20 I. Taniguchi, K. Kinugasa, M. Toyoda, K. Minezaki, H. Tanaka and K. Mitsuhara, *Polym. J.*, 2021, **53**, 129.
21 M. Henmi, K. Nakatsuji, T. Ichikawa, H. Tomioka, T. Sakamoto, M. Yoshio and T. Kato, *Adv. Mater.*, 2012, **24**, 2238.
22 T. Sakamoto, T. Ogawa, H. Nada, K. Nakatsuji, M. Mitani, B. Soberats, K. Kawata, M. Yoshio, H. Tomioka, T. Sasaki, M. Kimura, M. Henmi and T. Kato, *Adv. Sci.*, 2018, **5**, 1700405.
23 D. Kuo, M. Liu, K. R. S. Kumar, K. Hamaguchi, K. P. Gan, T. Sakamoto, T. Ogawa, R. Kato, N. Miyamoto, H. Nada, M. Kimura, M. Henmi, H. Katayama and T. Kato, *Small*, 2020, **16**, 202001721.
24 D. Kuo, T. Sakamoto, S. Torii, M. Liu, H. Katayama and T. Kato, *Polym. J.*, 2022, **54**, 821.
25 T. Sakamoto, K. Asakura, N. Kang, R. Kato, M. Liu, T. Hayashi, H. Katayama and T. Kato, *J. Mater. Chem. A*, 2023, **11**, 22178.
26 J. Uchida, B. Soberats, M. Gupta and T. Kato, *Adv. Mater.*, 2022, **34**, 2109063.
27 T. Kato, M. Yoshio, T. Ichikawa, B. Soberats, H. Ohno and M. Funahashi, *Nat. Rev. Mater.*, 2017, **2**, 17001.
28 K. Kishimoto, M. Yoshio, T. Mukai, M. Yoshizawa, H. Ohno and T. Kato, *J. Am. Chem. Soc.*, 2003, **125**, 3196.
29 K. Hoshino, M. Yoshio, T. Mukai, K. Kishimoto, H. Ohno and T. Kato, *J. Polym. Sci. Part A: Polym. Chem.*, 2003, **41**, 3486.
30 J. E. Bara, A. K. Kaminski, R. D. Noble and D. L. Gin, *J. Membr. Sci.*, 2007, **288**, 13.
31 J. Kloos, N. Jansen, M. Houben, A. Casimiro, J. Lub, Z. Borneman, A. P. H. J. Schenning and K. Nijmeijer, *Chem. Mater.*, 2021, **33**, 8323.
32 B. E. Jones, J. L. Greenfield, N. Cowieson, M. J. Fuchter and R. C. Evans, *J. Am. Chem. Soc.*, 2024, **146**, 12315.
33 T. Ichikawa, M. Yoshio, A. Hamasaki, J. Kagimoto, H. Ohno and T. Kato, *J. Am. Chem. Soc.*, 2011, **133**, 2163.
34 R. Watanabe, T. Sakamoto, K. Yamazoe, J. Miyawaki, T. Kato and Y. Harada, *Angew. Chem., Int. Ed.*, 2020, **59**, 23461.
35 Y. Ishii, N. Matubayasi, G. Watanabe, T. Kato and H. Washizu, *Sci. Adv.*, 2021, **7**, eabf0669.
36 S. Mehlhose, T. Sakamoto, M. Eickhoff, T. Kato and M. Tanaka, *J. Phys. Chem. B*, 2024, **128**, 4537.
37 Y. Zhang, R. Dong, U. R. Gabinet, R. Poling-Skutvik, N. K. Kim, C. Lee, O. Q. Imran, X. Feng and C. O. Osuji, *ACS Nano*, 2021, **15**, 8192.
38 T. Kai, S. Kazama and Y. Fujioka, *J. Membr. Sci.*, 2009, **342**, 14.
39 J. Liao, Z. Wang, C. Gao, S. Li, Z. Qiao, M. Wang, S. Zhao, X. Xie, J. Wang and S. Wang, *Chem. Sci.*, 2014, **5**, 2843.
40 Y. Li, Q. Xin, H. Wu, R. Guo, Z. Tian, Y. Liu, S. Wang, G. He, F. Pan and Z. Jiang, *Energy Environ. Sci.*, 2014, **7**, 1489.